

Dynamically generated open charmed baryons beyond the zero range approximation

C. E. Jiménez-Tejero¹, A. Ramos¹ and I. Vidaña²

¹*Departament d'Estructura i Constituents de la Matèria and Institut de Ciències del Cosmos, Universitat de Barcelona, Avda. Diagonal 647, E-08028 Barcelona, Spain and*

²*Centro de Física Computacional, Department of Physics, University of Coimbra, 3004-516 Coimbra, Portugal*

Abstract

The interaction of the low lying pseudo-scalar mesons with the ground state baryons in the charm sector is studied within a coupled channel approach using a t-channel vector-exchange driving force. The amplitudes describing the scattering of the pseudo-scalar mesons off the ground-state baryons are obtained by solving the Lippmann–Schwinger equation. We analyze in detail the effects of going beyond the $t = 0$ approximation. Our model predicts the dynamical generation of several open charmed baryon resonances in different isospin and strangeness channels, some of which can be clearly identified with recently observed states.

PACS numbers: 14.20.Lq, 14.40.Lb, 21.65.+f, 12.38.Lg

I. INTRODUCTION

A very active topic of research in hadron physics concerns the study and characterization of resonances, in order to establish whether they qualify as genuine $q\bar{q}$ or qqq states or, alternatively, they behave more as hadron molecules generated dynamically. A series of pioneer works [1, 2, 3, 4, 5, 6], based on a t -channel vector meson exchange force, already predicted a wealth of s -wave baryon resonances generated by coupled channel dynamics with effective hadronic degrees of freedom rather than quarks and gluons. The earlier approaches have been readapted in the last decade to the modern language of chiral lagrangians [7, 8, 9, 10, 11, 12, 13, 14, 15, 16, 17, 18, 19, 20, 21, 22, 23, 24] and many resonances in the light $SU(3)$ sector, which cannot be described properly by quark models [25] unless substantial meson-baryon components are included [26], have been identified with dynamical states generated from the interactions of mesons of the pseudoscalar 0^- octet with the $1/2^+$ ground state baryons. Some consequences of these studies, such as the two-pole nature of the $\Lambda(1405)$, are confirmed through the analyses [27, 28] of different experimental reactions [29, 30, 31]. Note that the basic structure of a molecular-type baryon is quite different from that implied by the quark models, even when they include the dressing with meson-baryon components, as in the 3P_0 formalism, where the qqq Hilbert space is coupled to the meson-baryon Hilbert space through the creation of a $q\bar{q}$ pair [32, 33, 34, 35, 36, 37]. In the former case the degrees of freedom are purely hadronic and the resonances must be seen as pseudo-bound states of two hadrons, while in the later case the essential component of a baryon is still of three quark nature. A goal in hadron physics research is to distinguish between both pictures from thorough analyses of as many properties of the hadron as possible, such as the mass, width, magnetic moment, form-factors, etc...

In recent years it was demonstrated that besides the s -wave baryon resonances many more states can be generated dynamically. Baryon resonances with $J^P = 3/2^-$ were studied based on the leading order chiral lagrangian with the decuplet $3/2^+$ fields [38, 39, 40, 41]. D -wave baryon resonances were also generated dynamically with vector meson degrees of freedom in Refs. [42, 43, 44, 45, 46, 47]. Another promising line of research is the recent interpretation of low lying $J^P = 1/2^+$ resonances as molecular states of two pseudoscalar mesons and one baryon [48, 49, 50, 51, 52]. All these results support the so-called hadrogenesis conjecture, formulated a few years ago by Lutz and Kolomeitsev, according to which resonances not belonging to the large- N_c ground state of QCD are generated by coupled-channel dynamics [18, 42, 53, 54, 55].

The study of charmed hadrons is receiving an increased attention thanks to the efforts of a

series of collaborations, both at lepton colliders (CLEO, BELLE, BaBar) and hadron facilities (CDF@Fermilab, PHENIX and STAR@RHIC, FAIR@GSI). The new results confirm with better statistics previously seen charmed states but are also giving rise to the discovery of a large amount of new hadrons [56, 57, 58, 59, 60, 61, 62, 63, 64, 65, 66, 67, 68, 69]. Coupled-channel unitary schemes have been recently extended to include the charm degree of freedom and have been applied to the description of open and hidden charm mesons, with the observation that some states admit a straightforward interpretation as meson molecules [70, 71, 72, 73, 74, 75]. Similar methods have been used for describing baryons with charm, motivated in part by a clear parallelism between the behavior of the $\Lambda(1405)$ in the $C = 0, S = -1$ sector with the $\Lambda_c(2595)$ in the $C = 1$ and $S = 0$ one [76, 77, 78, 79, 80, 81]. To be consistent with the spin-flavour Heavy Quark Symmetry that develops in this heavy sector [82, 83, 84], the vector mesons and $J = 3/2^+$ baryons have recently been included in the basis of meson-baryon states, employing a static spin-flavour SU(8) scheme [85] similar to that developed in the light sector [43, 44]. Treating the D and D^* mesons on an equal footing basis has led to the observation that some of the dynamical generated states, such as the $\Lambda_c(2595)$, have mostly a D^*N composition rather than the DN molecular nature. In any case, the observation that some of the dynamically generated charmed hadrons can be readily identified with observed resonances, such as the $J^P = 1/2^-$ $\Lambda_c(2595)$ or the $J^P = 3/2^-$ $\Lambda_c(2625)$ charmed baryons, sustains the hadrogenesis conjecture [18, 42, 53, 54, 55].

Apart from the different basis of states included in the models, a common feature of all the previous works is the use of an interaction based on the t -channel exchange of vector mesons, as the driving force for the s -wave scattering of pseudo-scalar mesons off ground state baryons. The limit $t \rightarrow 0$ is applied, leading to a vector type WT zero-range interaction. This procedure is justified for on-shell meson-baryon transitions, $MB \rightarrow M'B'$, which are diagonal ($M'B' = MB$) and hence the value of t is small as long as one is not too far from threshold. It also holds for non-diagonal amplitudes ($M'B' \neq MB$) that show a moderate difference of masses between the initial and final mesons and baryons involved, as is the case of meson-baryon scattering within the light SU(3) world. However, the coupled channel dynamics in the heavy sector finds also charm-exchange processes for which the difference of masses between the external mesons are comparable with the mass of the charmed vector meson being exchanged. This clearly signals the breakdown of the zero-range approximation which is no longer reliable for these non-diagonal transitions. While one may still argue that many of the dynamically generated states are triggered by a single dominant meson-baryon interaction component and, hence, their energy can be well estimated by the pole position of an uncoupled calculation involving only diagonal amplitudes, the corresponding width

will however be determined by non-diagonal amplitudes and will therefore depend on whether the $t = 0$ approximation is implemented or not. Moreover, it is well known that some resonances owe their origin to a particularly strong coupling between different channels, hence involving non-diagonal transitions, in which case the $t = 0$ approximation is not at all appropriate for these states.

In the present work we study the charmed baryon resonances obtained dynamically from the interaction of the low lying pseudo-scalar mesons with the ground state baryons within a coupled channel approach, using the full t -dependence of the t-channel vector-exchange driving term, instead of the $t = 0$ approximation. We incorporate the t -dependence within a general four-dimensional integration scheme, which we reduce to a three-dimensional equation of the ‘‘Lippmann-Schwinger’’ type, and analyze in detail the effects of going beyond the $t = 0$ approximation within this scheme.

The paper is organized as follows. In Sec. II we present the formalism, showing the details of the kernel employed and the equation used to obtain the scattering amplitudes. Our results for the properties of the baryon resonances with charm in various strangeness and isospin cases are shown in Sec. III, where we also compare with the $t = 0$ results. A summary of our conclusions is presented in Sec. IV.

II. FORMALISM

Following the original work of Hofmann and Lutz [78], we identify a t-channel exchange of vector mesons as the driving force for the s-wave scattering. In their original model, Hofmann and Lutz exploited the universal vector meson coupling hypothesis. They considered the t-channel exchange of vector mesons between pseudoscalar mesons in 16-plet and baryons in 20-plet representations in such a way to respect chiral symmetry for the light meson sector. The Weinberg–Tomozawa type interaction is recovered in the zero range limit, (*i.e.*, $t \rightarrow 0$ and see Eqs. (6) and (8) of Ref. [78] for details). The scattering kernel has the form

$$V_{ij}^{(I,S,C)}(k_i, q_i, k_j, q_j) = \frac{g^2}{4} \sum_{V \in [16]} C_{ij;V}^{(I,S,C)} \bar{u}(p_j) \gamma^\mu \left(g_{\mu\nu} - \frac{(q_i - q_j)_\mu (q_i - q_j)_\nu}{m_V^2} \right) \frac{1}{t - m_V^2} (q_i + q_j)^\nu u(p_i), \quad (1)$$

where the sum runs over all vector mesons of the SU(4) 16-plet, (ρ , K^* , \bar{K}^* , ω , ϕ , D^* , D_s^* , \bar{D}^* , \bar{D}_s^* , J/Ψ), m_V is the mass of the exchanged vector meson, g is the universal vector meson coupling constant, k_i, q_i, k_j and q_j are the four momenta of the incoming and outgoing baryon and

meson, and the coefficients $C_{ij;V}^{(I,S,C)}$ denote the strength of the interaction in the different sectors ($I, S, C = 1$) and channels (i, j). The value of $g = 6.6$ reproduces the decay width of the rho meson [86].

Assuming that $|t/m_V^2| \ll 1$, the t -dependence of the scattering kernel can be neglected, giving rise to the zero-range approximation. The s-wave projection of the scattering kernel under such approximation is easily obtained, and in the center-of-mass frame it takes the form

$$V_{ij,l=0}^{(I,S,C)}(k_i, q_i, k_j, q_j) = -N \frac{g^2}{4} \sum_{V \in [16]} \frac{C_{ij;V}^{(I,S,C)}}{m_V^2} \left(\omega(|\vec{k}_i|) + E(|\vec{k}_i|) + \omega(|\vec{k}_j|) + E(|\vec{k}_j|) - M_i - M_j - \frac{m_j^2 - m_i^2}{m_V^2} (M_i - M_j) \right), \quad (2)$$

where m_i, m_j, M_i, M_j are the masses of the incoming and outgoing mesons and baryons, and $\omega_i(|\vec{k}_i|), \omega_j(|\vec{k}_j|), E_i(|\vec{k}_i|), E_j(|\vec{k}_j|)$ their corresponding energies, which have been taken to be their on-shell values. The factor $N = [(E(|\vec{k}_i|) + M_i)(E(|\vec{k}_j|) + M_j)/(4M_i M_j)]^{1/2}$ comes from the normalization of the Dirac spinors. Note that for physical (fully on-shell) transition amplitudes one has $\omega_i(|\vec{k}_i|) + E_i(|\vec{k}_i|) = \omega_j(|\vec{k}_j|) + E_j(|\vec{k}_j|) = \sqrt{s}$, in which case one recovers the familiar expression of the commonly used Weinberg–Tomozawa interaction. The last term in Eq. (2) is usually ignored in most works, to be more consistent with the $t = 0$ approximation applied in the denominator of the meson-exchange propagator, as noted in Ref. [81]. In any case, its consideration introduces only minor corrections [78].

In order to illustrate the validity of this approach we show in Fig. 1 the value of t/m_V^2 for $\cos \theta = -1$ as a function of \sqrt{s} , where m_V is the mass of a representative meson exchanged, which we take to be the ρ meson mass for diagonal transitions and the D^* meson mass for charm exchange ones. The range of energies goes roughly between the $\pi\Sigma_c$ and DN thresholds, thereby covering the region of the $J^P = 1/2^-$ resonance $\Lambda_c(2595)$, which is a prime example of a dynamically generated open charmed baryon state in various approaches [76, 77, 78, 79, 80, 81]. It also expands beyond the DN threshold for about 300 MeV in order to explore the energy region that will be relevant in future studies of the D -meson self-energy in a nuclear medium. As one can see, the value of t/m_V^2 is only close to zero for diagonal transitions around their corresponding energy threshold, and its size can be comparable to one at the energies of interest. For the non-diagonal $\pi\Sigma_c \rightarrow DN$ transition, t/m_V^2 never goes to zero and acquires values of the order of 0.5.

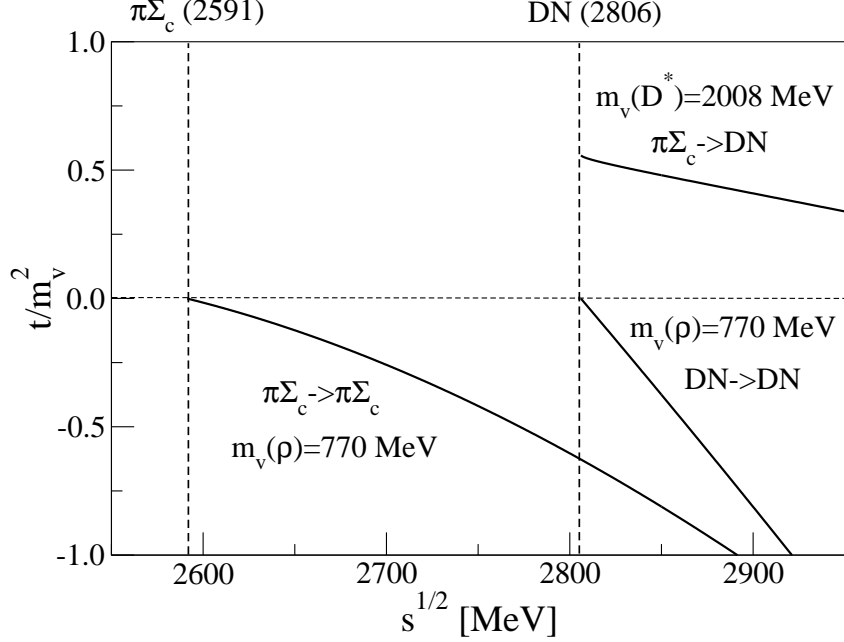


FIG. 1: Dependence on the center-of-mass energy \sqrt{s} of the four momentum transfer t/m_V^2 for $\cos\theta = -1$ and for different transition amplitudes.

The results of Fig. 1 point clearly to the need for exploring the effects of going beyond the $t = 0$ approximation, an attempt that is taken in the present work by considering the full t -dependence of the scattering kernel given by Eq. (1). Performing the s-wave projection, we obtain the following analytic expression:

$$V_{ij,l=0}^{(I,S,C)}(\vec{k}_i, \vec{k}_j) = N \frac{g^2}{8} \sum_{V \in [16]} C_{ij;V}^{(I,S,C)} \left[\frac{2\beta}{b} + \frac{\alpha b - \beta a}{b^2} \ln \left(\frac{a+b}{a-b} \right) \right], \quad (3)$$

with a, b, α and β being

$$\begin{aligned} a &= m_i^2 + m_j^2 - 2\omega_i(|\vec{k}_i|)\omega_j(|\vec{k}_j|) - m_V^2 \\ b &= 2|\vec{k}_i||\vec{k}_j| \\ \alpha &= \Omega_i(|\vec{k}_i|) + \Omega_j(|\vec{k}_j|) - M_i - M_j - \frac{m_j^2 - m_i^2}{m_V^2} (\Omega_j(|\vec{k}_j|) - \Omega_i(|\vec{k}_i|) + M_i - M_j) \\ \beta &= \frac{|\vec{k}_i||\vec{k}_j|}{(E_i(|\vec{k}_i|) + M_i)(E_j(|\vec{k}_j|) + M_j)} \left(\Omega_i(|\vec{k}_i|) + \Omega_j(|\vec{k}_j|) + M_i + M_j \right. \\ &\quad \left. - \frac{m_j^2 - m_i^2}{m_V^2} (\Omega_j(|\vec{k}_j|) - \Omega_i(|\vec{k}_i|) + M_j - M_i) \right), \quad (4) \end{aligned}$$

where we have defined $\Omega(|\vec{k}|) \equiv \omega(|\vec{k}|) + E(|\vec{k}|)$.

The $t = 0$ expression of the s-wave interaction is recovered by expanding the logarithm of Eq. (3) in the limit $b/a \rightarrow 0$ up to the linear term in b/a , and setting $a = -m_V^2$. As one can infer from the

values of t/m_V^2 displayed in Fig. 1, keeping the t -dependence in the denominator of the kernel [see Eq. (1)] will decrease the strength of the diagonal transitions, since in this case $t < 0$. Therefore, in order to reproduce a given resonance found in local models, the present approach will in general need to compensate the lack of strength with a higher value of the cut-off momentum used to regularize the loop integrals. On the other hand, non-diagonal amplitudes, responsible mainly for the decay width of the dynamically generated states, will be enhanced since they are characterized by a positive time-like t value due to the large mass difference between the mesons and baryons involved in the transition. As a consequence, our resonances will be wider than those found in the local models.

Retaining the t -dependence in the kernel implies additional analytical structures [87] which prevent us from obtaining the scattering amplitudes by solving the Bethe-Salpeter (BS) equation using on-shell amplitudes only. Instead, we incorporate the t -dependence within a more general four-dimensional integration scheme, which we reduce to a three-dimensional equation of the ‘‘Lippmann-Schwinger’’ type. To this end, for a given value of the total scattering energy, we will evaluate the transition potential between any arbitrary pair of relative momenta within the cut-off value, keeping the dependence on the momentum transfer in the corresponding matrix element. This procedure follows the same spirit of the usual meson-exchange models of the NN interaction [88], also applied to meson-baryon scattering models [89, 90]. We note that keeping the full t dependence in the exchanged meson propagator also implies that retardation effects are implemented as done in the three-dimensional reduction of the Bethe-Salpeter equation of Ref. [91], which is different than the prescription based on time-dependent perturbation theory [88]. Both choices differ in the way off-shell effects are implemented and their differences in the NN sector show up especially in the contributions of the two-meson exchange box diagrams [88] not included in the present model. In any case, observables can be matched to experimental data with either choice of retardation effects by selecting appropriate values of the renormalization parameters.

We note that Eqs. (1) to (3) assume infinitely lived (zero width) exchanged vector mesons, while some of them have large widths due to their strong decay into a pair of mesons, like the ρ meson contributing to diagonal channels. We have checked, however, that the value of t is never larger than the square of the minimum energy required for the meson to decay, namely $(2m_\pi)^2$ in the case of ρ exchange or $(m_\pi + m_K)^2$ for K^* . In other words, the mesons being exchanged in this problem are largely off-shell and they will be treated as stable particles.

Once the scattering kernel has been constructed, we can obtain the T -matrices which describe the scattering of the pseudo-scalar meson fields off the baryon fields by solving the well known

Lippmann–Schwinger equation

$$T_{ij,l=0}^{(I,S,C)}(\vec{k}_i, \vec{k}_j, \sqrt{s}) = V_{ij,l=0}^{(I,S,C)}(\vec{k}_i, \vec{k}_j) + \sum_m \int \frac{d\vec{k}}{(2\pi)^3} F(|\vec{k}|) V_{im,l=0}^{(I,S,C)}(\vec{k}_i, \vec{k}) J_m(\sqrt{s}, \vec{k}) T_{mj,l=0}^{(I,S,C)}(\vec{k}, \vec{k}_j, \sqrt{s}) \quad (5)$$

where

$$J_m^{(I,S,C)}(\sqrt{s}, \vec{k}) = \frac{M_m}{2E_m(|\vec{k}|)\omega_m(|\vec{k}|)} \frac{1}{\sqrt{s} - E_m(|\vec{k}|) - \omega_m(|\vec{k}|) + i\eta} . \quad (6)$$

We have introduced a dipole-type form factor $F(|\vec{k}|)$

$$F(|\vec{k}|) = \left(\frac{\Lambda^2}{\Lambda^2 + |\vec{k}|^2} \right)^2 \quad (7)$$

to regularize the integral. This form is typically adopted in studies of hadron-hadron interactions within the scheme of Lippmann-Schwinger-type equations in the light flavour sector [88]. The value of the cut-off Λ is a free parameter of our model. Given the limited amount of data for charmed baryon resonances, and in order to simplify the analysis, the cut-off Λ is adjusted to the position of a well known $J^P = 1/2^-$ state in a particular isospin and strangeness sector, and the same value is used for the other sectors explored in this work. We will also investigate the effect of a gaussian-type form factor, as well as the dependence of our results on the value of the cut-off employed.

Note that the approaches based on the Bethe–Salpeter equation solved with on-shell amplitudes ignore the off-shellness (momentum dependence) of the kernel and scattering amplitude in the loop function. Actually, the on-shell factorization can only be justified within the WT form of the potential which is obtained after applying the $t \rightarrow 0$ limit.

Another aspect worth commenting is the different extrapolation of the kernel at subthreshold energies. While the kernel of the on-shell BS approaches depends on \sqrt{s} in the form given by Eq. (2) upon replacing $\omega_i(|\vec{k}_i|) + E_i(|\vec{k}_i|) + \omega_j(|\vec{k}_j|) + E_j(|\vec{k}_j|)$ by $2\sqrt{s}$, the potential used in the tri-dimensional Lippmann–Schwinger equation depends essentially on the incoming and outgoing tri-momenta. These are always taken real quantities in our approach, hence the sum of the four single particle energies is always larger than the sum of the two meson-baryon thresholds involved in the transition. An explicit dependence on \sqrt{s} is only implemented in the meson-baryon intermediate propagator of the Lippmann–Schwinger equation that determines the scattering amplitudes. Therefore, at subthreshold energies, the factor in the numerator of the kernel used in on-shell BS approaches is smaller than in the present work. This in part compensates the enhancement in diagonal transitions associated to the $t \rightarrow 0$ limit. In any case, the free parameters of the model

(cut-off values) can finally be conveniently fine-tuned to adjust the energy position of a well known resonance, as is usually done for the case of the $\Lambda_c(2595)$ appearing about 200 MeV below the threshold of the channel DN to which it couples very strongly. In this respect, the differences between the present work and the on-shell BS approaches will be made more evident in properties tied to non-diagonal transitions which are reduced in the $t \rightarrow 0$ limit, as is the case of the resonance widths.

In order to associate a given enhancement of the scattering amplitude to a resonance, we look for a characteristic pole in the unphysical sheet of the complex energy plane. Our prescription of unphysical sheet is such that, whenever the real part of the complex energy crosses a meson-baryon threshold cut, the sign of the on-shell momentum is changed for this channel and for the already opened ones, as described in detail in Ref. [4]. Once a pole z_R is found, its value determines the Breit-Wigner mass ($M = \text{Re } z_R$) and width ($\Gamma = 2 \text{Im } z_R$) of the resonance, as seen from real energies, if the pole is not too far from the real axis. The couplings of the resonances into the meson-baryon components of a given sector are obtained from the residues of the scattering amplitude since, close to the pole, it can be parameterized in the form:

$$T_{ij,l=0}^{I,S,C}(\vec{k}_i, \vec{k}_j, z) = \frac{g_i g_j}{z - z_R} . \quad (8)$$

Note that, as it stands, the value of the coupling constants of Eq. (8) depend on the particular momentum values chosen in the evaluation of the T -matrix element. Since we are only interested on the size of the couplings relative to the various channels, we take the prescription of evaluating them for the case $\vec{k}_i = \vec{k}_j = 0$.

III. RESULTS AND DISCUSSION

One of the main interests of this paper is to study the effects of going beyond the $t = 0$ approximation in the kernel, as has been customarily done. We have already anticipated in the previous section that, in the case of coupled channel problems involving light and heavy flavored particles, this approximation is not always justified.

All the possible sectors with charm $C = 1$ that can be built from the s-wave scattering of pseudoscalar mesons with $J^P = 1/2^+$ baryons are shown in Table I, together with the corresponding meson-baryon coupled channels. In this work, we will first study the cases in which some resonance with either $J^P = 1/2^-$ or unknown spin-parity has already been observed. This includes the sectors with isospin, strangeness quantum numbers $(I, S) = (0, 0)$, $(1, 0)$ and $(1/2, -1)$, corresponding

$(\frac{1}{2}, -3, 1)$	$\bar{K}\Omega_c$
$(0, -2, 1)$	$\bar{K}\Xi_c \bar{K}\Xi'_c D\Xi \eta\Omega_c \eta'\Omega_c \bar{D}_s\Omega_{cc} \eta_c\Omega_c$
$(1, -2, 1)$	$\pi\Omega_c K\Xi_c K\Xi'_c D\Xi_c$
$(\frac{1}{2}, -1, 1)$	$\pi\Xi_c \pi\Xi'_c \bar{K}\Lambda_c \bar{K}\Sigma_c D\Lambda \eta\Xi_c D\Sigma \eta\Xi'_c K\Omega_c D_s\Xi \eta'\Xi_c \eta'\Xi'_c \eta_c\Xi_c \bar{D}_s\Xi_{cc} \bar{D}\Omega_{cc} \eta_c\Xi'_c$
$(\frac{3}{2}, -1, 1)$	$\pi\Xi_c \pi\Xi'_c \bar{K}\Sigma_c D\Sigma$
$(0, 0, 1)$	$\pi\Sigma_c DN \eta\Lambda_c K\Xi_c K\Xi'_c D_s\Lambda \eta'\Lambda_c \eta_c\Lambda_c \bar{D}\Xi_{cc}$
$(1, 0, 1)$	$\pi\Lambda_c \pi\Sigma_c DN K\Xi_c \eta\Sigma_c K\Xi'_c D_s\Sigma \eta'\Sigma_c \bar{D}\Xi_{cc} \eta_c\Sigma_c$
$(2, 0, 1)$	$\pi\Sigma_c$
$(\frac{1}{2}, 1, 1)$	$K\Lambda_c D_sN K\Sigma_c$
$(\frac{3}{2}, 1, 1)$	$K\Sigma_c$

TABLE I: Coupled-channel meson-baryon states with charm $C = 1$ and all possible combinations of isospin, strangeness (I,S).

respectively to Λ_c , Σ_c and Ξ_c states, the experimental information of which is gathered in Table II. We will next explore the sector $(I, S) = (0, -2)$ of the Ω_c states which so far has no experimental evidences for $J^P = 1/2^-$ states. Finally, we will comment on the $(I, S) = (1/2, 1)$ sector that can only be realized with the presence of 5 quarks.

Resonance [MeV]	$I(J^P)$	Width [MeV]	Decay modes	Status
$\Lambda_c(2595)^+$	$0(\frac{1}{2}^-)$	$3.6_{1.3}^{+2.0}$	$\Lambda_c\pi\pi, \Sigma_c\pi$	***
$\Lambda_c(2765)^+$ or $\Sigma_c(2765)$	$?(?)$	~ 50	$\Lambda_c\pi\pi$	*
$\Lambda_c(2940)^+$	$0(?)$	17_{-6}^{+8}	$ND, \Sigma_c\pi$	***
$\Sigma_c(2800)$	$1(?)$	$75_{-17}^{+22}(\Sigma_c^{++}), 62_{-40}^{+60}(\Sigma_c^+), 61_{-18}^{+28}(\Sigma_c^0)$	$\Lambda_c\pi$	***
$\Xi_c(2790)$	$\frac{1}{2}(\frac{1}{2}^-)$	$< 15(\Xi_c^+), < 12(\Xi_c^0)$	$\Xi'_c\pi$	***
$\Xi_c(2930)$	$?(?)$	36 ± 13	$\Lambda_c K$	*
$\Xi_c(2980)$	$\frac{1}{2}(?)$	$26 \pm 7(\Xi_c^+), 20 \pm 7(\Xi_c^0)$	$\Lambda_c\bar{K}\pi, \Sigma_c\bar{K}$	***
$\Xi_c(3055)$	$?(?)$	17 ± 13	$\Lambda_c\bar{K}\pi, \Sigma_c\bar{K}$	**
$\Xi_c(3080)$	$\frac{1}{2}(?)$	$5.8 \pm 1.0(\Xi_c^+), 5.6 \pm 2.2(\Xi_c^0)$	$\Lambda_c\bar{K}\pi, \Sigma_c\bar{K}, \Sigma_c^*\bar{K}$	***
$\Xi_c(3123)$	$?(?)$	4 ± 4	$\Sigma_c^*\bar{K}$	*

TABLE II: Masses, widths, decay modes and status of experimental charmed baryon resonances with $J^P = 1/2^-$ or unknown.

A. Λ_c resonances ($I=0, S=0, C=1$) sector

In this sector there exists a three-star narrow $J = 1/2^-$ resonance, the $\Lambda_c(2595)$, which has been extensively studied in various works [76, 78, 79, 80, 81]. We start by comparing in Fig. 2 the results obtained using our non-local kernel with those taking the limit $t \rightarrow 0$. We represent the imaginary part of the scattering amplitude of the elastic process $DN \rightarrow DN$, as a function of \sqrt{s} for zero incoming and outgoing relative momentum values. We can see that, by adjusting the cut-off value conveniently, both models of the kernel can generate this state dynamically. However, the zero range approximation needs a cut-off value of $\Lambda = 553$ MeV while the finite range interaction requires a substantially larger value of $\Lambda = 903$ MeV.

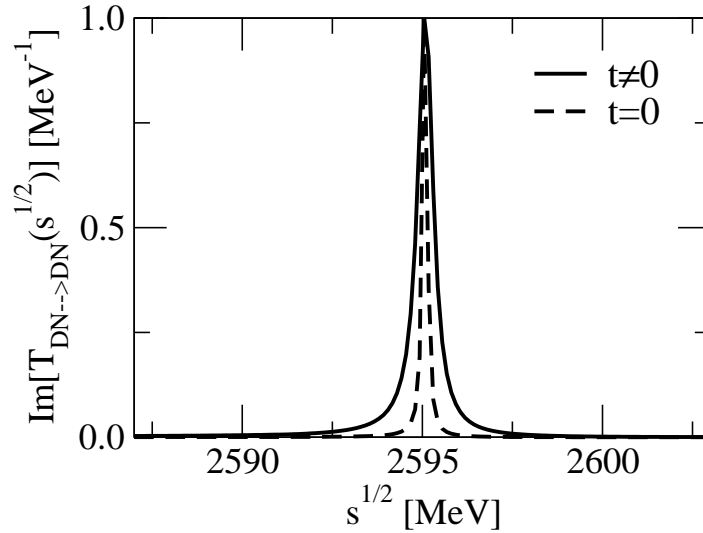


FIG. 2: Imaginary part of the scattering amplitude of the elastic process $DN \rightarrow DN$ in the $(I, S, C) = (0, 0, 1)$ sector as a function of \sqrt{s} for the finite range interaction (solid line) and the zero range approximation (dashed line). The incoming and outgoing relative momenta \vec{k}_i and \vec{k}_j have been taken equal to 0.

This is easily understood from the fact that the $DN \rightarrow DN$ diagonal matrix elements of the non-local potential, largely responsible for generating the resonance, are smaller in magnitude than those of the local one. The large difference between the cut-off momentum values is just a reflection of the importance of the non-local terms in this problem. Once the $\Lambda_c(2595)$ resonance is conveniently located to its experimental position by both prescriptions, there remain substantial differences in its width. The local potential produces a very narrow resonance, of width 0.15 MeV, while the resonance generated by the finite range potential has a width of 0.5 MeV, closer to the empirical value of $3.6 + 2.0 - 1.3$ MeV. Again, this is due to the different magnitude of the non-diagonal matrix elements $DN \rightarrow \pi\Sigma_c$, which are larger in the finite range approach. We note that

our model does not consider the three-body decay channel $\Lambda_c\pi\pi$ which already represents almost one third of the decay events [86]. We also observe that the results obtained with the low cut-off in the approximation $t = 0$ for the $\Lambda_c(2595)$ agree (mass, width and couplings) with former studies of meson-baryon resonances of Hofmann and Lutz in Ref. [78] and Garcia-Recio *et al.*, in Ref. [85].

Our search of resonances in this sector produces two states that are listed in Table III, together with their widths and couplings to the various meson baryon states. We immediately see that the $\Lambda_c(2595)$ is basically a DN state which couples very weakly to its only possible decaying channel $\pi\Sigma_c$, thereby explaining its narrowness. We obtain an even narrower resonance at 2805 MeV, which is a $K\Xi_c$ bound system, a state also found around the same energy in Ref. [78] and Ref. [85]. Note that this resonance couples non-negligibly to DN and, was its location be moved upward in energy by 20–30 MeV with a slight change of the cut-off parameter, it could explain part of the structures seen below 2.85 GeV in the D^0p invariant mass spectrum measured by the BaBar collaboration [68]. Table III also shows the results obtained with the local $t = 0$ model. We remark that, in spite of the fact that the second resonance appears at a higher energy, 2827 MeV, its width is narrower than in the finite-range model, confirming the trend observed for the $\Lambda_c(2595)$.

$(I = 0, S = 0, C = 1)$				
Λ [MeV]	903 ($t \neq 0$)	553 ($t = 0$)		
M [MeV]	2595	2805	2595	2827
Γ [MeV]	0.5	0.01	0.15	0.006
Couplings $ g_i $				
$\pi\Sigma_c(2591)$	0.44	0.001	0.21	0.002
$DN(2806)$	16.34	0.23	18	0.03
$\eta\Lambda_c(2832)$	0.58	1.92	0.22	1.60
$K\Xi_c(2963)$	0.71	3.76	0.23	3.22
$K\Xi'_c(3070)$	0.32	0.004	0.01	0.13
$D_s\Lambda(3085)$	8.16	0.18	8.54	0.07
$\eta'\Lambda_c(3243)$	0.96	0.01	0.54	0.003
$\eta_c\Lambda_c(5265)$	2.83	0.02	1.74	0.007
$\bar{D}\Xi_{cc}(5307)$	0.07	0.96	0.03	0.48

TABLE III: Masses, widths and couplings of the resonances in the $(I, S, C) = (0, 0, 1)$ sector, for the non-local ($t \neq 0$) and local ($t = 0$) models.

We represent in Fig. 3 the modulus square of the coherent sum of all transition amplitudes

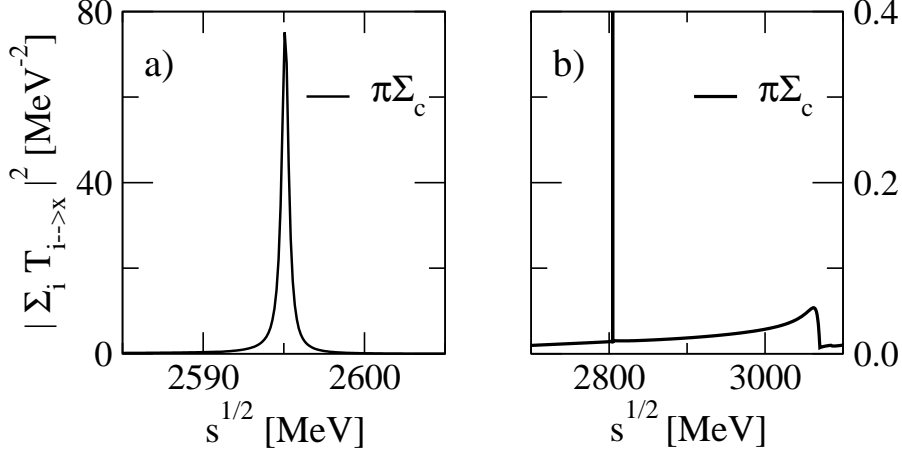


FIG. 3: Modulus square of the coherent sum of all transition amplitudes going to any of the possible final meson-baryon decaying channels, as a function of \sqrt{s} , for the $(I, S, C) = (0, 0, 1)$ sector. Our results are split into two panels, covering different energy regions and having different energy scales, to better visualize the properties of each state. The incoming and outgoing relative momenta \vec{k}_i and \vec{k}_j have been taken equal to 0.

going to a final meson-baryon state to which the resonances can decay, namely:

$$\sum_{M'B'} |C_{M'B'}^R T_{M'B' \rightarrow MB}(\sqrt{s})|^2, \quad (9)$$

where the values of the coefficients $C_{M'B'}^R$ would depend on the specific reaction used to excite the resonance and, in this graphical example, have all been taken to one. The amplitudes have been calculated for zero incoming and outgoing relative momentum values. To compare to actual experiments, one should be using the appropriate excitation coefficients as well as transition matrix elements going to the on-shell final momentum corresponding to the value of \sqrt{s} . Therefore, the results in Fig. 3 and similar ones throughout the paper should be considered merely illustrative. The representation is split into the various energy regions where the resonances appear. In general, a resonance couples dominantly to a given channel and the value of the maximum of Eq. (9) is basically proportional to the modulus squared of the product of the resonance couplings to the dominant and decaying channels, $g_{M'B'}$ and g_{MB} respectively, and inversely proportional to the resonance width Γ . Note that, instead of adjusting the vertical axis of Fig. 3b to the maximum associated to the narrow resonance at 2805 MeV, we have scaled it down to better visualize the enhancement at 3069 MeV, right below the $K\Xi'_c$ threshold. This enhancement becomes a resonance if we increase the cut-off value slightly, with properties that are similar to the state found around the same energy by the local models [78, 85].

B. Σ_c resonances: ($I=1, S=0, C=1$) sector

$(I = 1, S = 0, C = 1)$				
Λ [MeV]	903 ($t \neq 0$)		553 ($t = 0$)	
M [MeV]	2551	2804	2585	2804
Γ [MeV]	0.15	5	0.005	0.63
Couplings $ g_i $				
$\pi\Lambda_c(2424)$	0.06	0.27	0.002	0.04
$\pi\Sigma_c(2591)$	4.00	0.16	2.15	0.04
$DN(2806)$	1.25	2.10	0.38	1.70
$K\Xi_c(2963)$	0.04	0.20	0.003	0.06
$\eta\Sigma_c(2999)$	0.79	0.11	0.44	0.03
$K\Xi'_c(3070)$	2.30	0.14	1.55	0.04
$D_s\Sigma(3162)$	0.62	1.79	0.17	1.37
$\eta'\Sigma_c(3410)$	0.04	0.19	0.006	0.09
$\bar{D}\Xi_{cc}(5307)$	0.91	0.15	0.30	0.02
$\eta_c\Sigma_c(5432)$	0.13	0.55	0.02	0.27

TABLE IV: Masses, widths and couplings of the resonances in the $(I, S, C) = (1, 0, 1)$ sector, for the non-local ($t \neq 0$) and local ($t = 0$) models.

Using the same cut-off that reproduces the $\Lambda_c(2595)$ in the $(I, S, C) = (0, 0, 1)$ sector, we predict two narrow resonances at 2551 and 2804 MeV that appear right below the thresholds of the channels to which they couple mostly, namely $\pi\Sigma_c$ and DN , respectively, as can be seen from Table IV. We also show the results obtained with the $t = 0$ model and the same cut-off value of $\Lambda = 553$ MeV adjusted to the position of the $\Lambda_c(2595)$ in the isoscalar channel. As expected, the resonance at 2804 MeV, which couples mostly to DN states, barely changes its position from that of the non-local model. Indeed, since the $\Lambda_c(2595)$ also couples mostly to DN , the cut-off adjustment of the local model using this resonance as reference has essentially left the DN amplitude intact in this energy region, thereby generating similar “DN-type” bound states as in the non-local model in the various isospin sectors. Note, however, that the width of the resonance at 2804 MeV is an order of magnitude smaller in the local model. The lower energy resonance, coupling mostly to $\pi\Sigma_c$ states, appears at somewhat larger energies in the local model and, in spite of the gain in phase space, its width is substantially reduced. This comparison confirms the trend already observed in the case of the $I = 0$ sector. The resonances of the local model appear at similar energies as those

of the non-local approach but their widths are much smaller. Since this will be a general behavior in all sectors, we will only show, in the remaining sections, the results obtained with the non-local approach developed in this work.

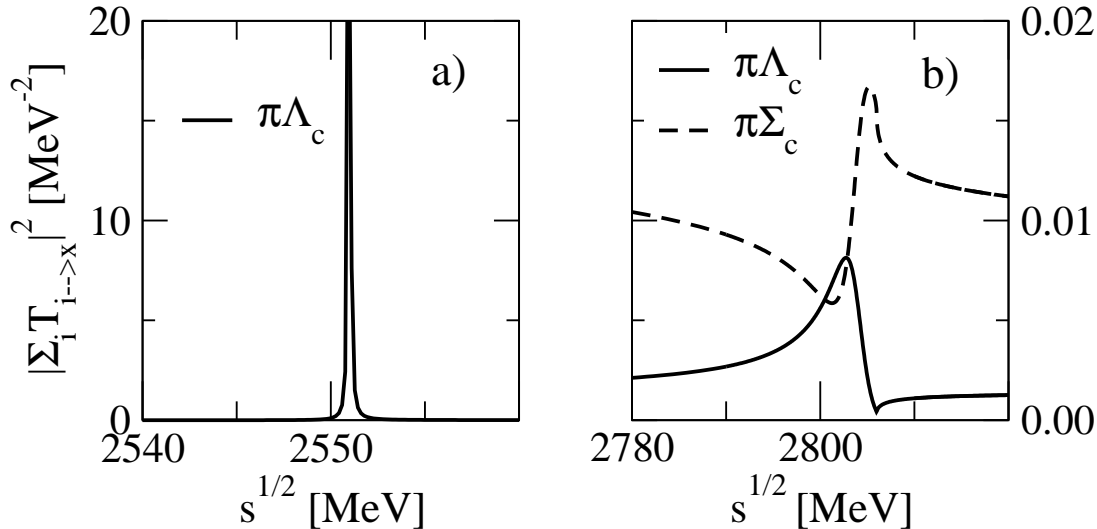


FIG. 4: The same as Fig. 3 but for the $(I, S, C) = (1, 0, 1)$ sector.

The sum of amplitudes squared is represented in Fig. 4. Since the $\Sigma_c(2551)$ resonance couples negligibly to its only allowed strong decaying channel, $\pi\Lambda_c$, it is seen in Fig. 4a as a narrow peak which makes it easy to miss given the energy resolution of the meson-baryon invariant masses built up in the present experiments. The couplings to the different meson-baryon states of the Σ_c resonance at 2804 MeV, visualized in Fig. 4b, allow one to identify it with the state found in Ref. [78] at a substantially lower energy, 2680 MeV, using a subtraction method to regularize the loops, as well as that found in Ref. [81] around 2750 MeV, using a cut-off method which preserves isospin symmetry in the regularization scheme. Our result is obviously closer to that of the latter work.

The Belle Collaboration reported recently [62] an isotriplet of excited charmed baryons, $\Sigma_c(2800)$, decaying into $\Lambda_c^+\pi^-$, $\Lambda_c^+\pi^0$ and $\Lambda_c^+\pi^+$ pairs and having a width of around 60 MeV with more than 50% error. Although this resonance has been tentatively assumed to decay to $\Lambda_c\pi$ pairs in d-wave and its spin parity estimated to be $J^P = 3/2^-$, actual angular distributions have not been measured and the fits to $\Lambda_c\pi$ spectra can not rule out s-wave type decays. Hence, our state at 2805 MeV could be easily identified with the $\Sigma_c(2800)$ resonance, provided three-body decay mechanisms not accounted for in our model, could explain the large width observed experimentally.

C. Ξ_c resonances: ($\mathbf{I}=1/2, \mathbf{S}=-1, \mathbf{C}=1$) sector

The results in this sector are presented in Table V and Fig. 5. We obtain two pure bound states at 2515 and 2549 MeV, respectively, which are placed less than one pion mass above the Ξ_c member of the $J^P = 1/2^+$ ground state antitriplet, $(\Lambda_c^+, \Xi_c^+, \Xi_c^0)$, and below the mass of the Ξ_c' member of the $J^P = 1/2^+$ sextet, $(\Sigma_c^0, \Sigma_c^+, \Sigma_c^{++}, \Xi_c'^0, \Xi_c'^+, \Omega_c^0)$. This implies that these bound states would decay electromagnetically through the emission of $\Xi_c \gamma$ pairs and may have been detected at photon energies of about 50 and 80 MeV in the experiment where the Ξ_c' was observed [63]. Although no apparent signals are reported, we note that the limited statistical significance of the spectra measured in [63] prevents one from ruling out the existence of these bound states. Moreover, their production rate would also be somewhat inhibited by the fact that they are predominantly 5 quark-component states. Note also that, lowering gradually the value of the cut-off to somewhat below 700 MeV, the first state at 2515 MeV eventually becomes resonance, but quite narrow due to its weak coupling to the first channel, whereas the second state at 2549 MeV, which is a $\pi \Xi_c$ molecule, rapidly becomes so wide that it would be difficult to be distinguished from the background.

In addition, our model gives three more resonances above the $\pi \Xi_c$ threshold and below 3 GeV, placed at 2733, 2840 and 2977 MeV. The local model of Ref. [78], based on on-shell amplitudes, also obtains three resonances in this energy region, located in general at somewhat lower masses and showing a different order of appearance, as can be inferred from the values of their couplings to the different meson-baryon components. More specifically, the lowest resonance in the local model appearing at 2691 MeV and coupling strongly to $D\Sigma$ should be identified with our middle resonance at 2840 MeV. The next two resonances appear quite close in the scheme of Ref. [78], at 2793 MeV and 2806 MeV, coupling mostly to $\bar{K}\Sigma_c$ and $D\Lambda$, respectively, while in our case they are further apart from each other, at 2733 and 2977 MeV. The crossing in the ordering of states is another consequence of the different values of the transition potential amplitudes used in both coupled-channel schemes.

Recently, several Ξ_c states have been observed by the CLEO [64], Belle [65] and BaBar [66] Collaborations, out of which the three star possible candidates to be identified with one of our states are at 2790, 2980 and 3080 MeV [see Table II]. A change of the cut-off value within a reasonable range could bring any of our two lower mass resonances to agree in position with the $\Xi_c(2790)$ but the width would turn out to be twice wider than the observed one in the case of the lower mass state. The $\Xi_c(2980)$ could be easily associated to either one of the two higher mass states found here. However, the experimental analysis of Ref. [66] concludes that the $\Xi_c(2980)^+$

$(I = 1/2, S = -1, C = 1)$					
M [MeV]	2515	2549	2733	2840	2977
Γ [MeV]	0.	0.	34	0.58	4
Couplings $ g_i $					
$\pi\Xi_c(2609)$	0.65	4.47	0.05	0.06	0.31
$\pi\Xi'_c(2715)$	4.84	0.76	1.77	0.01	0.22
$\bar{K}\Lambda_c(2779)$	0.48	3.21	0.19	0.10	0.19
$\bar{K}\Sigma_c(2946)$	6.90	1.01	7.37	0.93	0.16
$D\Lambda(2985)$	1.03	0.30	0.96	1.54	2.95
$\eta\Xi_c(3018)$	0.13	1.04	0.13	0.18	0.10
$D\Sigma(3062)$	2.91	0.89	3.64	8.82	1.74
$\eta\Xi'_c(3124)$	4.04	0.59	3.47	0.46	0.07
$K\Omega_c(3192)$	4.40	0.68	1.47	0.07	0.21
$D_s\Xi(3288)$	1.74	0.15	0.92	4.71	2.51
$\eta'\Xi_c(3428)$	0.16	0.05	0.15	0.53	0.06
$\eta'\Xi'_c(3534)$	0.01	0.03	0.09	0.11	0.28
$\bar{D}_s\Xi_{cc}(5408)$	0.02	0.01	0.25	0.35	0.71
$\bar{D}\Omega_{cc}(5429)$	1.10	0.53	1.18	0.24	0.03
$\eta_c\Xi_c(5450)$	1.17	1.10	0.55	0.04	0.03
$\eta_c\Xi'_c(5556)$	0.04	0.08	0.26	0.33	0.82

TABLE V: Masses, widths and couplings of the resonances in the $(I, S, C) = (\frac{1}{2}, -1, 1)$ sector

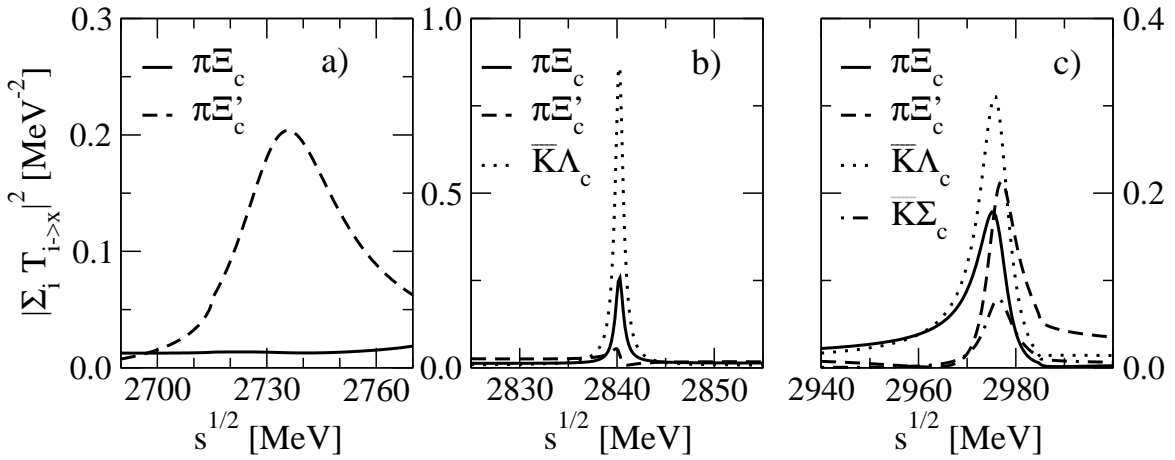


FIG. 5: The same as Fig. 3 but for the $(I, S, C) = (1/2, -1, 1)$ sector.

state decays in about 50% of the cases into $\Sigma_c^{++}K^-$ pairs, which makes our state at 2840 MeV, showing a stronger coupling to $\bar{K}\Sigma_c$, the most likely candidate to be associated to the $\Xi_c(2980)$.

D. Ω_c resonances: ($I=0, S=-2, C=1$) sector

In this sector we predict the existence of a bound state at 2959 MeV, near the lowest threshold, and two resonances placed at 2966 and 3117 MeV as can be seen in Table VI and Fig. 6. The possible bound state could be detected through the decay into $\Omega_c\gamma$ states with photons of $E_\gamma = 260$ MeV in the center-of-mass frame. The resonance placed at 2966 MeV and seen in Fig. 6a is very narrow ($\Gamma = 1.1$ MeV) according to the low coupling of the resonance to the only channel in which it can decay ($\bar{K}\Xi_c$) and the little available phase space. The resonance at 3117 MeV with a width of $\Gamma = 16$ MeV, seen in Fig. 6b, is a $D\Xi$ molecule that can decay into $\bar{K}\Xi_c$ and $\bar{K}\Xi'_c$ states.

$(I = 0, S = -2, C = 1)$			
M [MeV]	2959	2966	3117
Γ [MeV]	0.	1.1	16
Couplings $ g_i $			
$\bar{K}\Xi_c(2964)$	1.36	0.43	0.51
$\bar{K}\Xi'_c(3070)$	2.04	4.49	0.27
$D\Xi(3189)$	2.03	1.68	5.34
$\eta\Omega_c(3246)$	1.67	3.69	0.24
$\eta'\Omega_c(3656)$	0.10	0.07	0.35
$D_s\Omega_{cc}(5528)$	0.17	1.17	0.19
$\eta_c\Omega_c(5678)$	0.28	0.21	1.03

TABLE VI: Masses, widths and couplings of the resonances in the $(I, S, C) = (0, -2, 1)$ sector

The work of Ref. [78] also finds three states but placed at lower energies, 2839, 2928 and 2953 MeV, which follows the trend observed for other sectors. The pattern of couplings to the various meson-baryon states also differs a little owing to the different interaction model used. The highest energy resonance in Ref. [78], coupling strongly to $\bar{K}\Xi'_c$ and $\eta\Omega_c$, would correspond to our middle one, while the lowest one in Ref. [78], coupling strongly to $D\Xi$, would be the equivalent to our resonance at higher energy.

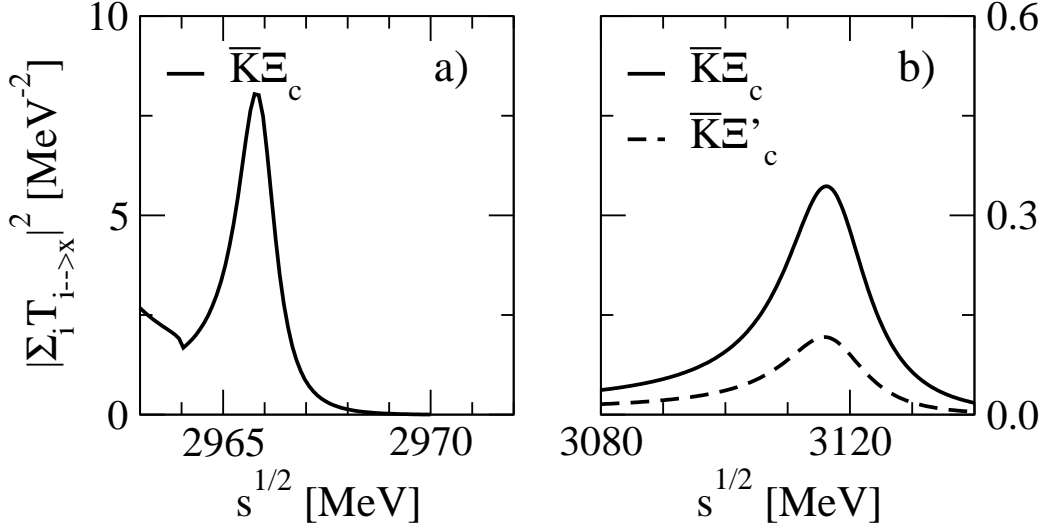


FIG. 6: The same as Fig. 3 but for the $(I, S, C) = (0, -2, 1)$ sector.

E. Resonances of five quarks

We have also analyzed the sectors corresponding to resonances that cannot be realized with only three quarks and, therefore, their existence would be signaling the presence of pure five quark states. Note that the possible pentaquark-type systems predicted by the present model would be color singlet states built up from combinations of color singlet $q\bar{q}$ with color singlet qqq components. States with a different composition, such as a combination of color octet $q\bar{q}$ with color octet qqq clusters, can not be generated by our meson-baryon scattering approach.

$(I = 1/2, S = 1, C = 1)$			
Λ [MeV]	903	1200	1400
M [MeV]	2946	2941	2924
Γ [MeV]	0.93	5	12
Couplings $ g_i $			
$K\Lambda_c(2779)$	0.002	0.04	0.10
$D_s N(2908)$	0.03	0.84	1.68
$K\Sigma_c(2946)$	0.07	1.79	3.59

TABLE VII: Masses, widths and couplings of the resonances in the $(I, S, C) = (1/2, 1, 1)$ sector for different cut-off values: 903, 1200 and 1400 MeV.

Out of the three possible sectors, namely $(I, S, C) = (2, 0, 1)$, $(\frac{1}{2}, 1, 1)$ and $(\frac{3}{2}, 1, 1)$, we only find hints of a possible resonance in the case $I = 1/2, S = 1, C = 1$, where we see a cusp-like

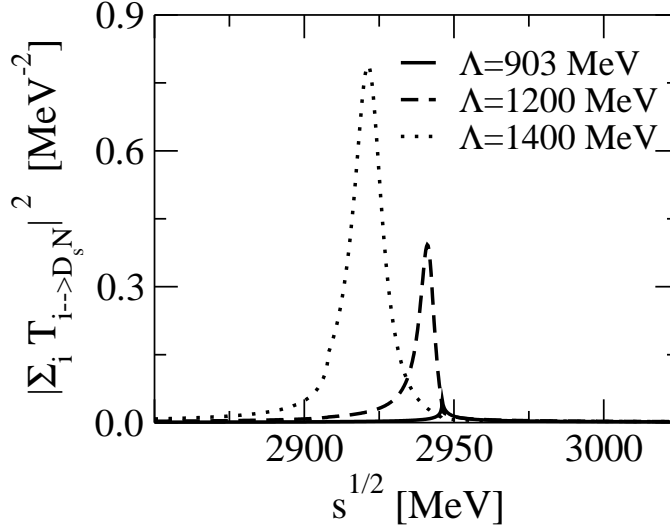


FIG. 7: The same as Fig. 3 but for the $(I, S, C) = (1/2, 1, 1)$ sector and for three different cut-off values: 903, 1200 and 1400 MeV.

structure placed at the threshold of the $K\Sigma_c$ channel to which the state couples more strongly. This behavior is shown by the solid line in Fig. 7 and by the first column of coupling constants displayed in Table VII, which have been obtained using our nominal cut-off value of 903 MeV. According to the mechanism discussed in Ref. [44], the coupling constants should vanish if the resonance was placed right at the $K\Sigma_c$ threshold, which explains the smallness of their values. In order to see whether the cusp structure would eventually become a clear resonance with a slight change of parameters, we also display in Fig. 7 and in Table VII our results with two other values of the cut-off, 1200 and 1400 MeV. One can clearly see that the cusp structure becomes a more bound and wider resonance as the cut-off value increases, while the coupling constants become larger.

F. Dependence on model parameters

We finalize this work by exploring the dependence of our results on the shape and size of the form factor employed, which are ingredients of the model that are not constrained by symmetry arguments.

First, replacing the dipole-type form factor by a gaussian form:

$$F(|\vec{k}|) = e^{-\frac{\vec{k}^2}{2\Lambda_g^2}},$$

we are able to adjust the position of the $\Lambda_c(2595)$ with a gaussian cut-off value of $\Lambda_g = 543$ MeV.

The corresponding width is exactly the same as that found for the dipole-type form factor. When exploring the other sectors, the gaussian form factor gives rise to the same resonances, some of them slightly displaced by at most 50 MeV from the position found with the dipole-type form factor, but having essentially the same width.

Retaining the dipolar form factor, we next explore the effects of varying the value of the cut-off Λ , a parameter that is not constrained by symmetry arguments, between 600 and 1200 MeV, that is, up to 300 MeV below and above the nominal value of 903 MeV used in this work. This variation produces changes in the positions and widths of the resonances within certain ranges, the general trend of which are summarized in the following points:

1. A resonance that lies far below –by 50 to 200 MeV– the meson-baryon threshold to which it couples more strongly may change its position by an amount comparable with the variation of the cut-off value. The larger the cut-off the more bound the resonance becomes.
2. The width of the resonance only changes appreciably for cut-off values that move the resonance above the threshold of a meson-baryon channel to which the resonance couples significantly.
3. Weakly bound resonances change their positions more moderately, at most by 10 MeV for changes of cut-off values within 100 MeV. In this case, the width tends to decrease as the resonance becomes less bound because of the distortions induced by moving closer to the threshold, a phenomenon also known as Flatté effect [92].

Having explored the systematics to the cut-off changes, we finally summarize in Table VIII the states which, taking an appropriate cut-off value within the range explored, could be identified with a well established resonance of $J^P = 1/2^-$ or unknown spin-parity.

IV. CONCLUSIONS

We have studied charmed baryon resonances obtained from a coupled channels unitary approach using a t-channel vector-exchange driving force.

To the best of our knowledge, all previous models of dynamically generated baryon resonances in the charm sector rely on a local zero-range interaction, which is obtained by neglecting the four-momentum transfer t in front of the mass of the exchanged vector meson squared, m_V^2 . However, we have illustrated that the value t/m_V^2 is not at all negligible in the heavy sector, especially for

(I, S)	Λ [MeV]	Theory			Experiment		
		Mass [MeV]	main channel	Width [MeV]	Mass [MeV]	Width [MeV]	Status
$(0, 0)$ Λ_c	903	2595	$DN(2806)$	0.5	2595.4 ± 0.6	$3.6_{1.3}^{+2.0}$	***
$(1, 0)$ Σ_c	1100	2792	$DN(2806)$	16	2801_{-6}^{+4} 2792_{-5}^{+14} 2802_{-7}^{+4}	75_{-17}^{+22} (Σ_c^{++}) 62_{-40}^{+60} (Σ_c^+) 61_{-18}^{+28} (Σ_c^0)	***
$(\frac{1}{2}, -1)$ Ξ_c	814 980 655 960	2790 2790 2970 2970	$\bar{K}\Sigma_c(2946)$ $D\Sigma(3062)$ $D\Sigma(3062)$ $D\Lambda(2980)$	55 0.5 1.2 5.1	2789.1 ± 3.2 2791.8 ± 3.3 2971.4 ± 3.3 2968.0 ± 2.6	< 15 (Ξ_c^+) < 12 (Ξ_c^0) 26 ± 7 (Ξ_c^+) 20 ± 7 (Ξ_c^0)	***

TABLE VIII: Masses, widths and main coupled channel of states that can be identified with well established resonances in various sectors.

charm-exchange amplitudes which produce a large value of the four-momentum transfer due to the large difference between the masses of the mesons involved in the transition.

We have analyzed in detail the effects of going beyond the $t = 0$ approximation and, taking the $I = 0, C = 1, J = 1/2$ sector of the well established $J = 1/2^-$ $\Lambda_c(2595)$ resonance as reference, we find that the experimental data is better reproduced by the non-local model which also requires a more reasonable cut-off regularization value of 903 MeV.

Compared to the local models based on on-shell amplitudes, our approach obtains basically the same amount of resonances in all sectors but appearing, in general, at somewhat larger energies because the diagonal amplitudes, largely responsible for generating the bound states, are smaller in magnitude. An essential finding of this work is that our non-local approach produces much wider resonances because of the larger value of the non-diagonal amplitudes when $t \neq 0$.

Varying the cut-off parameter within a reasonable range, we are able to locate some of our states at the energy position of a measured resonance in the same sector. In particular, we suggest the identification of the $\Lambda_c(2595)$, $\Sigma_c(2800)$, $\Xi_c(2790)$ and $\Xi_c(2980)$ as dynamically generated resonances having $J^P = 1/2^-$. In general, the widths of the states produced by our model are smaller than the experimentally observed ones, since we do not account for three-particle decay channels.

We find a possible resonance in the sector with quantum numbers $(I, S, C) = (\frac{1}{2}, 1, 1)$ that can

only be realized by the consideration of a minimum of five quarks. The cusp-like structure observed at the threshold of the $K\Sigma_c$ channel for a cut-off value of 903 MeV, becomes a more bound and wider clear resonance as the cut-off value increases.

This is the first exploratory study of the effects tied to the non-locality of the meson-baryon interaction in the charm sector. We have considered meson-baryon coupled states built up from the $J^P = 0^-$ mesons and the ground state $J^P = 1/2^+$ baryons. However, Heavy Quark Symmetry demands that the states containing heavy vector mesons are treated on equal footing due to the similarity of the masses with the heavy pseudoscalar ones. This will be addressed in a future work.

Acknowledgements

We are very grateful to M. F. M. Lutz for helpful discussions and comments. We also thank E. Graugés for clarifications on the details of the experiments, and B. Julià-Díaz, V.K. Magas and A. Parreño for interesting suggestions and their help in various stages of the calculation. This work is partly supported by the EU contract No. MRTN-CT-2006-035482 (FLAVIANet), by the contract FIS2008-01661 from MIC (Spain), by the Generalitat de Catalunya contract 2009SGR-1289, and by FEDER/FCT (Portugal) under the project CERN/FP/83505/2008. We acknowledge the support of the European Community-Research Infrastructure Integrating Activity “Study of Strongly Interacting Matter” (HadronPhysics2, Grant Agreement n. 227431) under the Seventh Framework Programme of EU.

-
- [1] J. S. Ball and W. R. Frazer, Phys. Rev. Lett. **7**, 204 (1961).
 - [2] H. W. Wyld, Phys. Rev. **155**, 1649 (1967).
 - [3] R. H. Dalitz, T. C. Wong and G. Rajasekaran, Phys. Rev. **153**, 1617 (1967).
 - [4] R. K. Logan and H. W. Wyld, Phys. Rev. **158**, 1467 (1967).
 - [5] G. Rajasekaran, Phys. Rev. D **5**, 610 (1972).
 - [6] P. S. Siegel and W. Weise, Phys. Rev. C **38**, 2221 (1988).
 - [7] N. Kaiser, P. B. Siegel and W. Weise, Nucl. Phys. A **594**, 325 (1995); N. Kaiser, P. B. Siegel and W. Weise, Phys. Lett. B **362**, 23 (1995); N. Kaiser, T. Waas and W. Weise, Nucl. Phys. A **612**, 297 (1997).
 - [8] J. Nieves and E. Ruiz Arriola, Phys. Rev. D **63**, 076001 (2001).
 - [9] C. Garcia-Recio, J. Nieves, E. Ruiz Arriola and M. J. Vicente Vacas, Phys. Rev. D **67**, 076009 (2003).
 - [10] A. Ramos, E. Oset and C. Bennhold, Phys. Rev. Lett. **89**, 252001 (2002).

- [11] E. Oset, A. Ramos and C. Bennhold, Phys. Lett. **B527**, 99(2002).
- [12] D. Jido, J. A. Oller, E. Oset, A. Ramos and U. G. Meissner, Nucl. Phys. A **725**, 181 (2003).
- [13] E. Oset and A. Ramos, Nucl. Phys. A **635**, 99 (1998).
- [14] U. G. Meissner and J. A. Oller, Nucl. Phys. A **673**, 311 (2000).
- [15] J. A. Oller, E. Oset and A. Ramos, Prog. Part. Nucl. Phys. **45**, 157 (2000).
- [16] J. A. Oller and U. G. Meissner, Phys. Lett. B **500**, 263 (2001).
- [17] J. Nieves and E. Ruiz Arriola, Phys. Rev. D **64**, 116008 (2001).
- [18] M. F. M. Lutz and E. E. Kolomeitsev, Nucl. Phys. A **700**, 193 (2002).
- [19] T. Inoue, E. Oset and M. J. Vicente Vacas, Phys. Rev. C **65**, 035204 (2002).
- [20] J. A. Oller, J. Prades and M. Verbeni, Phys. Rev. Lett. **95**, 172502 (2005).
- [21] B. Borasoy, R. Nissler and W. Weise, Eur. Phys. J. A **25**, 79 (2005).
- [22] B. Borasoy, U. G. Meissner and R. Nissler, Phys. Rev. C **74**, 055201 (2006).
- [23] T. Hyodo, D. Jido and A. Hosaka, Phys. Rev. C **78**, 025203 (2008).
- [24] T. Hyodo, D. Jido and L. Roca, Phys. Rev. D **77**, 056010 (2008).
- [25] S. Capstick and N. Isgur, Phys. Rev. D **34**, 2809 (1986).
- [26] P. Gonzalez, J. Vijande and A. Valcarce, Phys. Rev. C **77**, 065213 (2008).
- [27] V. K. Magas, E. Oset and A. Ramos, Phys. Rev. Lett. **95**, 052301 (2005).
- [28] D. Jido, E. Oset and T. Sekihara, arXiv:0904.3410 [nucl-th].
- [29] D. W. Thomas, A. Engler, H. E. Fisk, and R. W. Kraemer, Nucl. Phys. B **56**, 15 (1973).
- [30] S. Prakhov *et al.* [Crystal Ball Collaboration], Phys. Rev. C **70**, 034605 (2004).
- [31] O. Braun *et al.*, Nucl. Phys. B **129**, 1 (1977).
- [32] A. Le Yaouanc, L. Oliver, O. Pene, and J. C. Raynal, *Hadron Transitions of the Quark Model* (Gordon and Breach, Amsterdam, 1988).
- [33] R. Koniuk and N. Isgur, Phys. Rev. D **21**, 1868 (1980) [Erratum-ibid. D **23**, 818 (1981)].
- [34] N. A. Tornqvist and P. Zenczykowski, Phys. Rev. D **29**, 2139 (1984).
- [35] N. A. Tornqvist and P. Zenczykowski, Z. Phys. C **30**, 83 (1986).
- [36] W. Blask, M. G. Huber and B. Metsch, Z. Phys. A **326**, 413 (1987).
- [37] B. Silvestre-Brac and C. Gignoux, Phys. Rev. D **43**, 3699 (1991).
- [38] E. E. Kolomeitsev and M. F. M. Lutz, Phys. Lett. B **585**, 243 (2004).
- [39] S. Sarkar, E. Oset and M. J. Vicente Vacas, Nucl. Phys. A **750**, 294 (2005). [Erratum-ibid. A **780**, 78 (2006).]
- [40] L. Roca, S. Sarkar, V. K. Magas and E. Oset, Phys. Rev. C **73**, 045208 (2006).
- [41] M. Doring, E. Oset and D. Strottman, Phys. Lett. B **639**, 59 (2006).
- [42] M. F. M. Lutz, G. Wolf and B. Friman, Nucl. Phys. A **706**, 431 (2002).
- [43] C. García-Recio, J. Nieves and L. L. Salcedo, Phys. Rev. D **74**, 034025 (2006).
- [44] H. Toki, C. Garcia-Recio and J. Nieves, Phys. Rev. D **77**, 034001 (2008).
- [45] P. Gonzalez, E. Oset and J. Vijande, Phys. Rev. C **79**, 025209 (2009).

- [46] S. Sarkar, B. X. Sun, E. Oset and M. J. V. Vacas, arXiv:0902.3150 [hep-ph].
- [47] E. Oset and A. Ramos, arXiv:0905.0973 [hep-ph].
- [48] A. Martinez Torres, K. P. Khemchandani and E. Oset, Phys. Rev. C **77**, 042203 (2008).
- [49] A. Martinez Torres, K. P. Khemchandani and E. Oset, Eur. Phys. J. A **35**, 295 (2008).
- [50] K. P. Khemchandani, A. Martinez Torres and E. Oset, Eur. Phys. J. A **37**, 233 (2008).
- [51] D. Jido and Y. Kanada-En'yo, Phys. Rev. C **78**, 035203 (2008).
- [52] Y. Kanada-En'yo and D. Jido, Phys. Rev. C **78**, 025212 (2008).
- [53] M. F. M. Lutz and E. E. Kolomeitsev, Found. Phys. **31**, 1671 (2001).
- [54] M. F. M. Lutz, GSI-Habil-2002-1.
- [55] M. F. M. Lutz and E. E. Kolomeitsev, Nucl. Phys. A **730**, 392 (2004).
- [56] B. Aubert *et al.* [BaBar Collaboration], Phys. Rev. Lett. **90**, 242001 (2003).
- [57] D. Besson *et al.* [CLEO Collaboration], Phys. Rev. D **68**, 032002 (2003) [Erratum-ibid. D **75**, 119908 (2007)].
- [58] P. Krokovny *et al.* [Belle Collaboration], Phys. Rev. Lett. **91**, 262002 (2003).
- [59] S. K. Choi *et al.* [Belle Collaboration], Phys. Rev. Lett. **91**, 262001 (2003).
- [60] D. E. Acosta *et al.* [CDF II Collaboration], Phys. Rev. Lett. **93**, 072001 (2004).
- [61] M. Artuso *et al.* [CLEO Collaboration], Phys. Rev. Lett. **86**, 4479 (2001).
- [62] R. Mizuk *et al.* [Belle Collaboration], Phys. Rev. Lett. **94**, 122002 (2005).
- [63] C. P. Jessop *et al.* [CLEO Collaboration], Phys. Rev. Lett. **82**, 492 (1999).
- [64] S. E. Csorna *et al.* [CLEO Collaboration], Phys. Rev. Lett. **86**, 4243 (2001).
- [65] R. Chistov *et al.* [BELLE Collaboration], Phys. Rev. Lett. **97**, 162001 (2006).
- [66] B. Aubert *et al.* [BaBar Collaboration], Phys. Rev. D **77**, 012002 (2008).
- [67] B. Aubert *et al.* [BaBar Collaboration], Phys. Rev. Lett. **97**, 232001 (2006).
- [68] B. Aubert *et al.* [BaBar Collaboration], Phys. Rev. Lett. **98**, 012001 (2007).
- [69] R. Mizuk *et al.* [Belle Collaboration], Phys. Rev. Lett. **98**, 262001 (2007).
- [70] E. E. Kolomeitsev and M. F. M. Lutz, Phys. Lett. B **582**, 39 (2004).
- [71] J. Hofmann and M. F. M. Lutz, Nucl. Phys. A **733**, 142 (2004).
- [72] F. K. Guo, P. N. Shen, H. C. Chiang and R. G. Ping, Phys. Lett. B **641**, 278 (2006).
- [73] F. K. Guo, P. N. Shen and H. C. Chiang, Phys. Lett. B **647**, 133 (2007).
- [74] D. Gamermann, E. Oset, D. Strottman and M. J. Vicente Vacas, Phys. Rev. D **76**, 074016 (2007).
- [75] D. Gamermann and E. Oset, Eur. Phys. J. A **33**, 119 (2007).
- [76] M. F. M. Lutz and E. E. Kolomeitsev, Nucl. Phys. A **730**, 110 (2004).
- [77] M. F. M. Lutz and E. E. Kolomeitsev, Nucl. Phys. A **755**, 29c (2005).
- [78] J. Hofmann and M. F. M. Lutz, Nucl. Phys. A **763**, 90 (2005).
- [79] J. Hofmann and M. F. M. Lutz, Nucl. Phys. A **776**, 17 (2006).
- [80] L. Tolos, J. Schaffner-Bielich and A. Mishra, Phys. Rev. C **70**, 025203 (2004).
- [81] T. Mizutani and A. Ramos, Phys. Rev. C **74**, 065201 (2006).

- [82] N. Isgur and M.B. Wise, Phys. Lett. **B232**, 113 (1989).
- [83] M. Neubert, Phys. Rep. **245**, 259 (1994).
- [84] A.V. Manohar and M.B. Wise, *Heavy Quark Physics*, Cambridge Monographs on Particle Physics, Nuclear Physics and Cosmology, vol. 10, (Cambridge University Press, 2000).
- [85] C. Garcia-Recio, V. K. Magas, T. Mizutani, J. Nieves, A. Ramos, L. L. Salcedo and L. Tolos, Phys. Rev. D **79**, 054004 (2009).
- [86] C. Amsler *et al.* [Particle Data Group], Phys. Lett. B **667**, 1 (2008).
- [87] A. D. Lahiff and I. R. Afnan, Phys. Rev. C **66**, 044001 (2002).
- [88] R. Machleidt, K. Holinde and C. Elster, Phys. Rept. **149**, 1 (1987).
- [89] A. Mueller-Groeling, K. Holinde and J. Speth, Nucl. Phys. A **513**, 557 (1990); R. Buettgen, K. Holinde, A. Mueller-Groeling, J. Speth and P. Wyborny, Nucl. Phys. A **506**, 586 (1990); M. Hoffmann, J. W. Durso, K. Holinde, B. C. Pearce and J. Speth, Nucl. Phys. A **593**, 341 (1995).
- [90] J. Haidenbauer, G. Krein, U. G. Meissner and A. Sibirtsev, Eur. Phys. J. A **33**, 107 (2007).
- [91] F. Gross, Phys. Rev. **186**, 1448 (1969).
- [92] S.M. Flatté, Phys. Lett. **B63**, 224 (1976).